Journal of Applied Materials Engineering
2019, Vol. 59, Issue 3 (formerly PRACE INSTYTUTU ODLEWNICTWA)

Maps of crystal lattice orientation in polyphase microregions as a parameter of the microstructure image of a multicomponent metal alloy

Małgorzata Warmuzek[1] , Adelajda Polkowska[1]*

[1]ŁUKASIEWICZ – Foundry Research Institute, ul. Zakopiańska 73, 30-418 Krakow, Poland

**Corresponding author: malgorzata.warmuzek@iod.krakow.pl*

Received: 28.10.2019. Accepted in revised form: 13.12.2019. DOI: 10.7356/iod.2019.10

Abstract

This study includes the results of tests related to selecting the data collection parameters for EBSD analysis, correction and modification of the EBS diffraction patterns, and use of selected functionalities of the commercial OIM system. The study also shows the local misorientation range and the local relationships of the crystal lattice orientation at interfaces and grain boundaries, estimated in the polyphase microregions of selected AlFeMnSi alloys.

Keywords: intermetallic phase, crystal lattice, elementary cell, crystallographic orientation, SEM, EBSD

1. Introduction

Multicomponent aluminum-based metal alloys with transition metals crystallize to form a series of intermetallic phases [1]. Reactions involving intermetallic compounds in such alloys are mainly peritectic, and therefore occur very slowly, limited by the rate of diffusion of the individual elements [2]. The kinetics of peritectic crystallization is determined by the diffusion model of growth typical for long range order in the crystal lattice of intermetallics [3]. As the peritectic reactions usually do not reach their final stage in typical laboratory experiments, nonequilbrium phase composition is observed in the alloy microstructure after solidification finish. The mechanism of peritectic crystallization is characterized by two stages: reaction with participation of the liquid alloy and transformation without contact with the liquid alloy [4,5]. Advanced models of this process involve both peritectic reactions and transformations with the participation of solid solutions mainly in the Fe-C and Fe-Ni alloys [5,6]. Peritectic solidification in aluminum alloys has not been described completely until now in the literature. Some data can be found in works carried out in AlFeMnSi alloys [2,7], in which the solidification paths of two peritectic processes were analyzed with the participation of the cubic intermetallic phase, α_c-AlMnFeSi, as a peritectic phase and two other intermetallic phases, β_H-AlMnSi and Al_3Fe, as properitectic phases:

– $L + \beta_H\text{-AlMnSi} \rightarrow \alpha_c\text{-AlMnFeSi}$

– $L + Al_3Fe \rightarrow \alpha_c\text{-AlMnFeSi}$.

Both peritectic reactions mentioned above occur at the triple point: P1/L/α_c (where: L – liquid alloy, P1 – properitectic phase: β_H-AlMnS, or Al_3Fe, α_c – peritectic phase α_c-AlMnFeSi). Thus, the crystallographic relationships between two solid phases at the interfaces and at the triple point could be considered factors involved in the peritectic reaction. The factors controlling these interactions are still subject to examination, especially crystallographic determination of the morphological model of the three-phase peritectic reaction and its kinetic control.

Additionally, the crystal lattice relationships at the interfaces are taken into account as a factor controlling the heterogenic nucleation processes [8−10] involved in technical alloy casting [11] and other technological processes, such as recycling of aluminum scrap [12,13].

Therefore this work has two main aims:

– Development of an analytical procedure for recording and indexing phase maps and estimation of the misorientation degree at the interfaces depending on the crystal lattice and chemical composition in the polyphase microregions in selected AlFeMnSi alloys.

– Interaction analysis between the intermetallic phases involved in peritectic reactions in multiphase microregions controlled by crystallographic relationships between the primary and peritectic phases

in aluminum alloys with Si, Fe, and Mn, when the cubic α_c-AlFeMnSi is a peritectic phase.

2. Materials

The materials examined were AlFeMnSi alloys characterized by different ratio of the transition metals content, Fe/Mn. As a factor determining the solidification path of the alloy, and especially the type of preperytectic phase, differentiation in the value of the Fe/Mn ratio was assumed.

The chemical composition of the examined alloys is shown in Table 1.

Table 1. Chemical composition of the examined alloys (wt.%, Al bal.)

Alloy	Specimen no.	Fe	Mn	Si	Fe/Mn
33	1	3.6	4.0	2.6	0.9
6.05	2	10.6	8.5	4.7	1.2
7.5	3	9.1	3.0	3.0	3
25	4	9.1	0.7	2.7	19

3. Examinations

The following examinations were carried out:

– microstructure observations by AxioObserver 10Zm light microscope (LM) and SCIOS scanning electron microscope (SEM);

– *in situ* analyses: EDS x-ray microanalysis (EDAX, TEAM system), EBSD pattern analysis (Hikari camera, TEAM system);

– collection of phase maps and orientation maps, their modification and analysis (Hikari camera, TEAM system).

The analysis of crystal lattice misorientation between the intermetallic phases particles was carried out using phase maps recorded by the TEAM system and orientation analysis by the OIM system [15]. The analysis conditions were reviewed to optimize the results resolution, analysis time, and drift impact. The standard camera parameters and background optimization were used as the initial conditions.

4. Examination results

4.1. Microstructure observations

The microstructure of the examined alloys is shown in Figure 1.

As can be seen in Figure 1, in the examined alloys the polyphase microstructure formed during solidification. Two-phase, complex microregions were observed in all the examined specimens, characteristic for the intermediate stage of the peritectic reaction with the participation of two intermetallic phases. In the center of the two-phase particle the properitectic phase was located, while the peritectic phase formed its envelope.

4.2. Estimation of the chemical composition of the phase constituents of the examined alloys

The chemical compositions of the selected microregions in the examined alloy are shown in Table 2.

Table 2. Chemical composition of the selected microregions (wt.%, Al-bal.)

Specimen no.	Properitectic phase				Peritectic phase			
	Fe	Mn	Si	Fe/Mn	Fe	Mn	Si	Fe/Mn
1	21.6	11.0	9.6	1.9	16.5	15.6	7.7	1.1
2	38.2	3.1	3.9	12.3	19.9	12.1	9.4	1.6
3	37.4	3.9	4.2	9.6	21.6	11	9.6	2.0
4	40.1	1.5	3.0	26.7	30.0	2.1	5.3	15

It was found that in the intermetallic phases examined in selected microregions there were changes in the Fe/Mn ratio, depending on the original Fe/Mn ratio in the examined alloys. This is a typical tendency observed in Al-based alloys with the transition metals Fe and Mn, both synthetic [1,7,11] and technical [11−13].

4.3. Results of identification of the phase constituents

The phase constituents in the selected microstructure microregions were identified based on the EBSD diffraction patterns [14,15], indexed according to the standard patterns for the anticipated phase constituents (Fig. 2). The quality of the solution for the particular indexed pattern was estimated based on the value of the Confidence Index (CI), given automatically by the analytical system. The solutions with CI > 0.1 were taken into account for further consideration. In some cases an improvement in the CI value was possible by using a modified standard pattern, better matched to the actual crystal lattice in the analyzed microregion.

The phases recognized in the analyzed microregions are given in Table 3. Taking into account the peritectic reaction mechanism, the microregion situated at the center of the two-phase microregion was ascribed to the properitectic phase, while that peripheral to it was ascribed to the peritectic phase. The phase attributions, based on the EBS diffraction pattern, were in accordance with the results of previous work [2,7], literature data [16−19] and confirmed by local chemical composition, as shown in Table 2.

Table 3. The intermetallic phases recognized in the examined specimens

Specimen	Properitectic phase	Peritectic phase
1	β_H-AlFeMnSi	α_c-AlFeMnSi
2	Al_3Fe	α_c-AlFeMnSi
3	Al_3Fe	α_c-AlFeMnSi
4	Al_3Fe	α_c-AlFeMnSi

The results of the local, point phase identification were used as a base for further analyses, when phase maps were recorded in selected microregions.

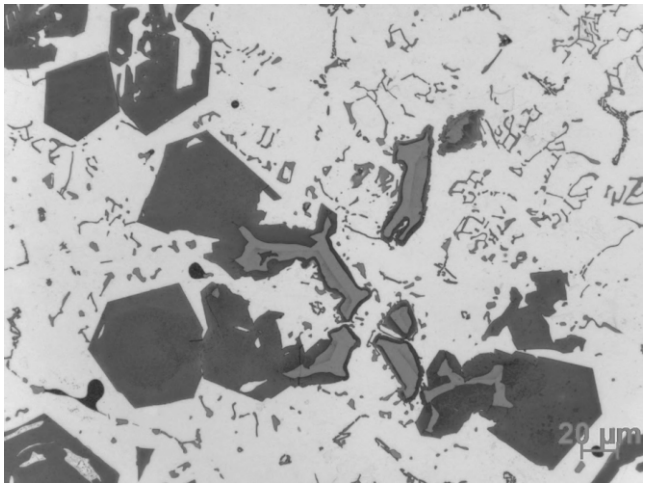

a)

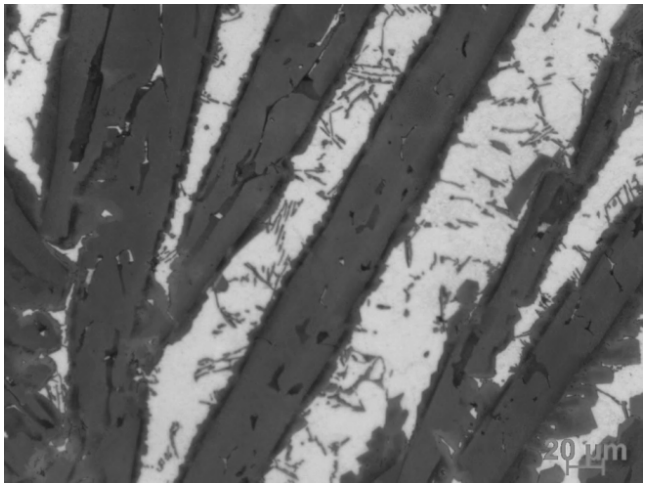

b)

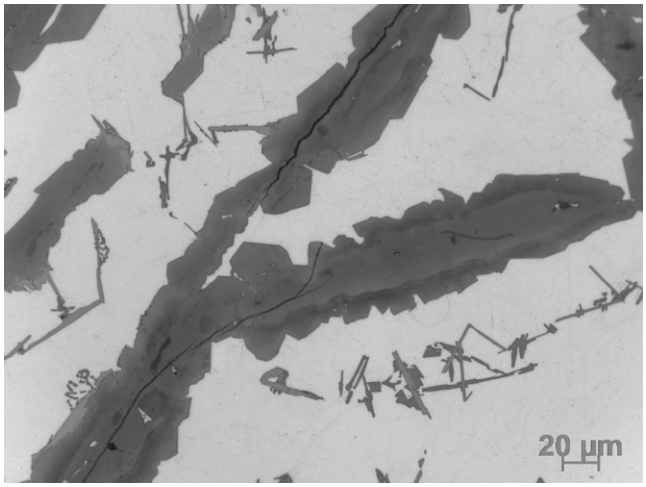

c)

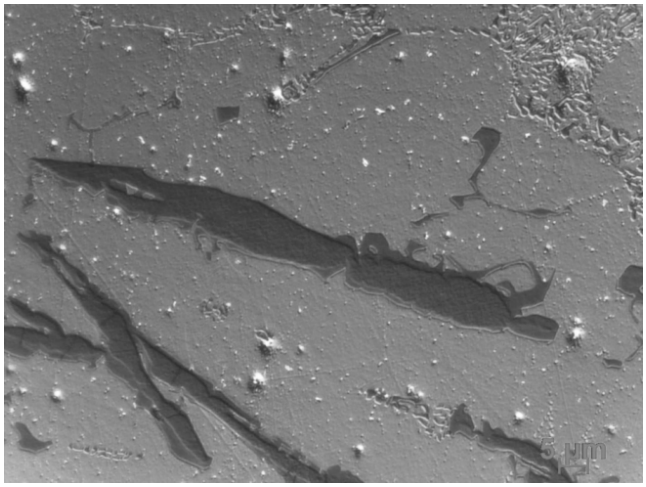

d)

Fig. 1. Microstructure of the examined specimens, microregion with intermetallic phases, peritectic and properitectic, polyphase residual eutectics; LM BF, a) specimen 1 (intermetallic phases: β_H-AlMnSi (center) and α_c-AlMnFeSi (envelope), b) specimen 2, (intermetallic phases: Al_3Fe (center) and α_c-AlMnFeSi (envelope), c) specimen 3, (intermetallic phases: Al_3Fe (center) and α_c-AlMnFeSi (envelope), d) specimen 4, (intermetallic phases: Al_3Fe (center) and α_c-AlMnFeSi (envelope)

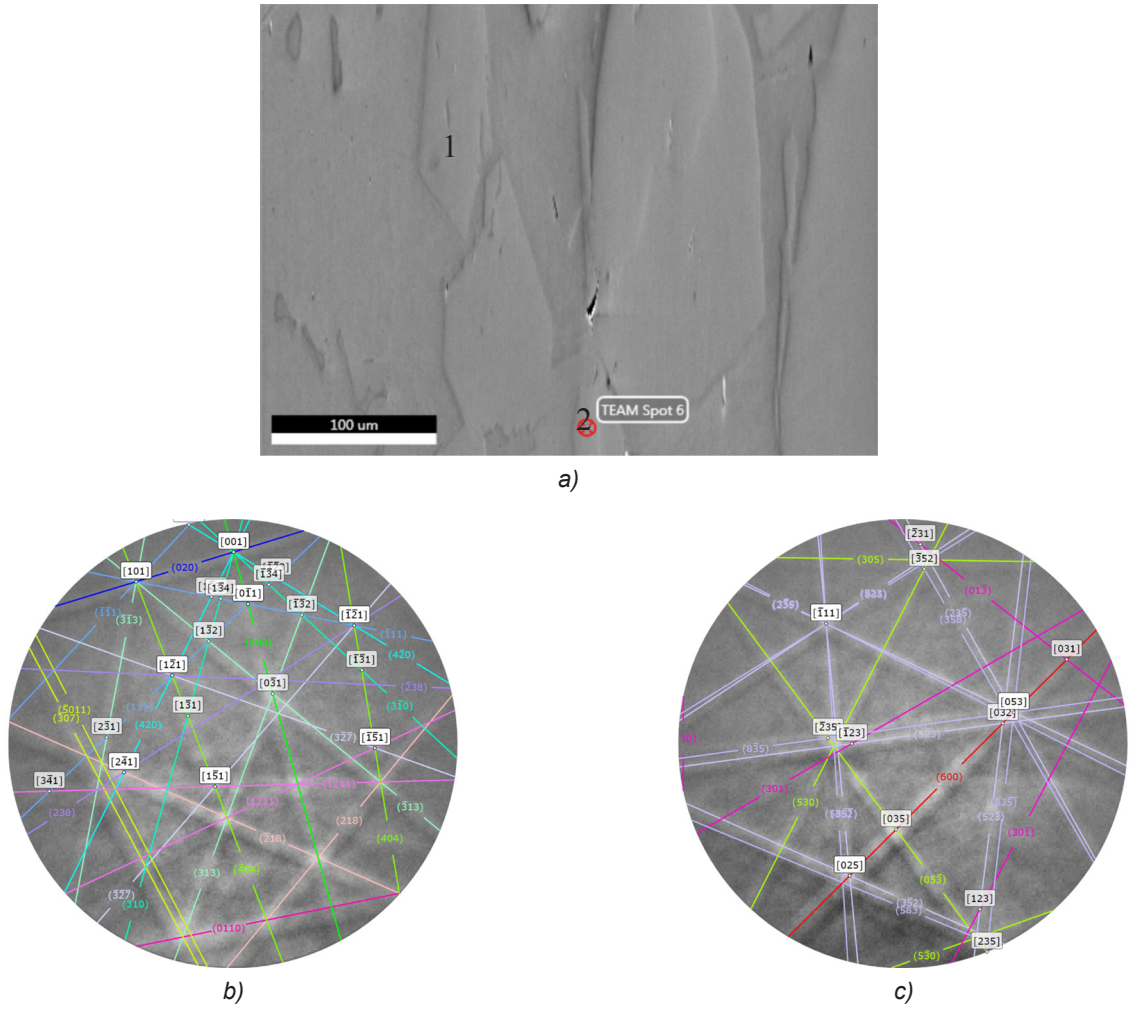

Fig. 2. Specimen 3: a) microstructure in the analyzed microregion, b) EBS diffraction pattern at point 1 in Fig. 3a, indexed for Al_3Fe, phase CI 0.18, c) EBS diffraction pattern at point 2 in Fig. 3a, indexed for α_c-AlFeMnSi, phase CI 0.5

4.4. Results of the analysis of crystal lattice misorientation between the intermetallic phase crystals

The complementary data of the phase distribution and local orientation relationships at the interfaces were recorded in the selected polyphase microregions containing a matrix, and crystals of two intermetallic phases, properitectic and peritectic, for each of the examined specimens. The collected maps give the type of phase constituents, their chemical compositions and actual crystallographic orientations (Fig. 3). The phase maps were recorded in these selected microregions, based on the phase constituents recognized previously by point EBSD analysis (Fig. 2).

4.5. Effect of the cleaning procedures on both phase and orientation maps

The recorded maps were modified and filtered to obtain clearer images. The results of the applied filtering procedure are shown in Figure 4 for the phase maps and Figure 5 for the orientation maps.

The filtering procedure eliminated most of the incorrectly assigned points in the phase maps (Fig. 4b). The crystals of each phase present in the analyzed microregion became more clearly visible. A similar result was obtained for the orientation map shown in Figure 5. The dispersion of the local orientations of the crystal lattice assigned to the crystal of a particular phase decreased, which made further analysis more effective.

4.6. Analysis of the orientation maps

Based on the cleaned datasets, the misorientation degree between two selected crystals, either of the same phase or of different phases, was estimated using a functionality of the OIM system. Examples of the results are shown in Figures 6−9.

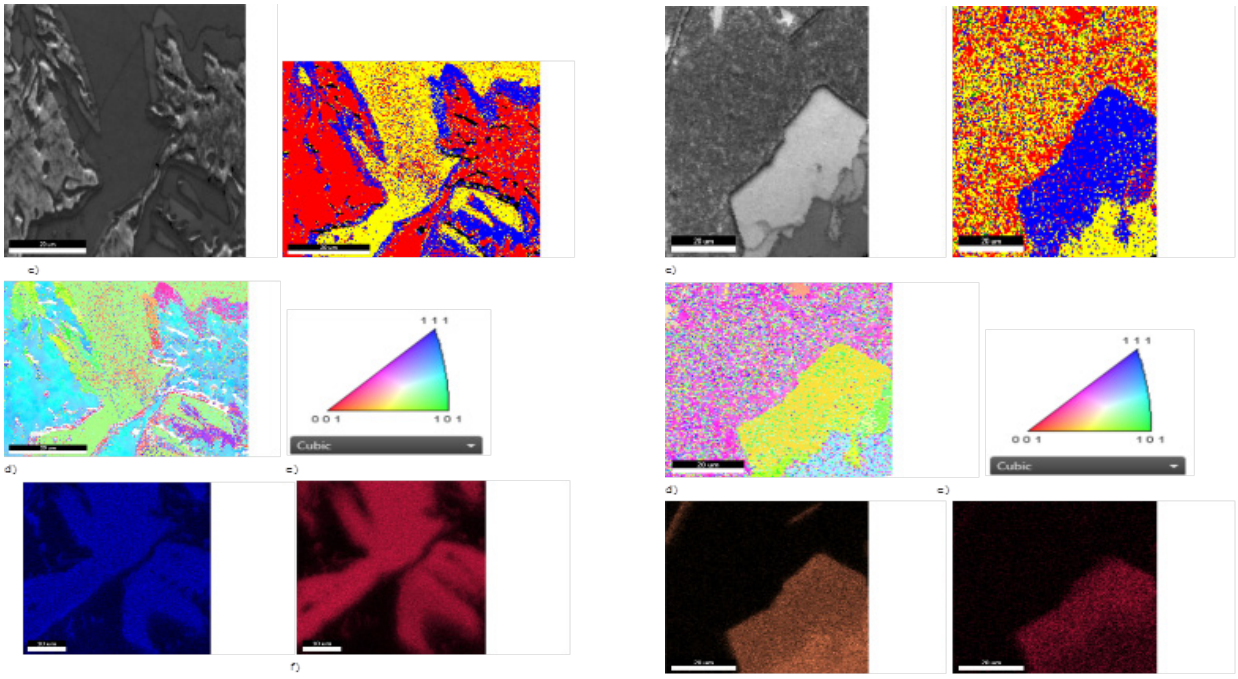

a) b)

Fig. 3. Example dataset recorded for the analyzed microregion: microstructure morphology, phase map, orientation map, distribution map of the main elements: a) specimen 1, b) specimen 3

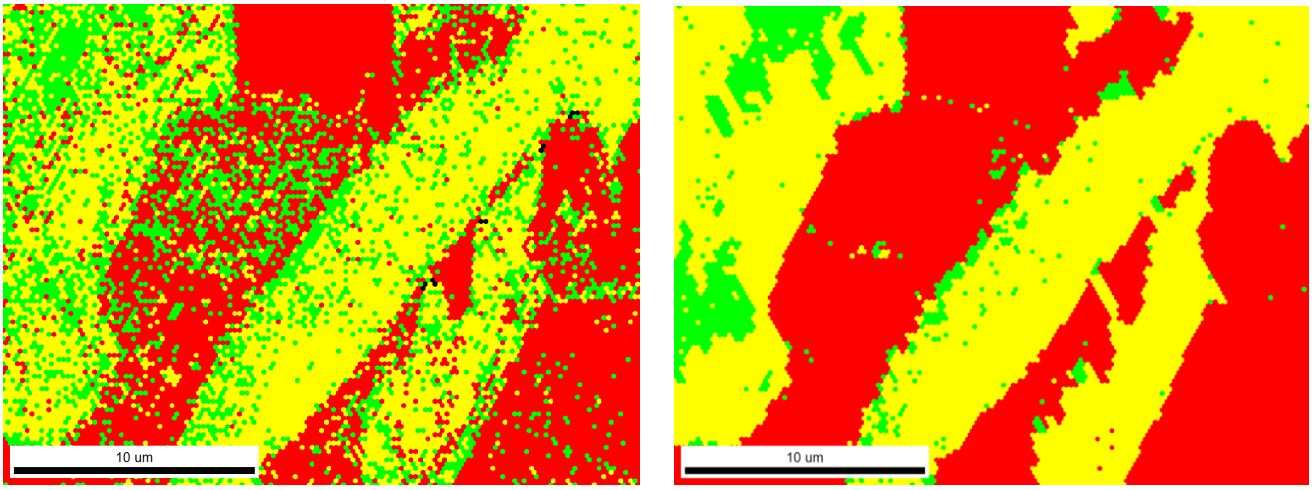

a) b)

Fig. 4. Specimen 1. Phase map in the selected microregion: a) initial map, recorded in situ, TEAM system, b) map after cleaning procedure, OIM system; identified phases: α_c-AlFeMnSi (red), β_H-AlFeMnSi (yellow), α-Al (green)

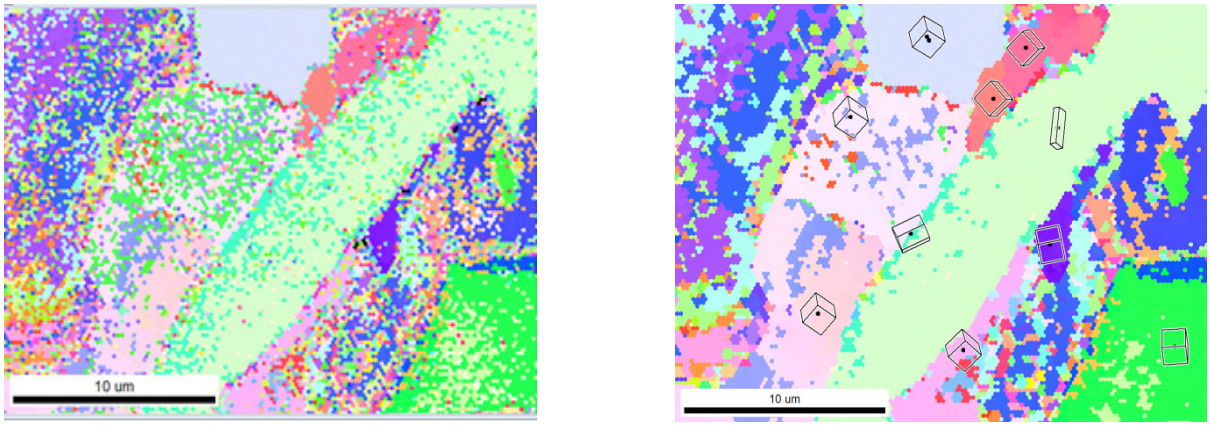

a) b)

Fig. 5. Specimen 1. Map of relative orientation between individual crystals: a) initial map recorded in situ, TEAM system, b) map after the cleaning procedure, OIM system, the local orientation of the elementary cell is shown at selected points

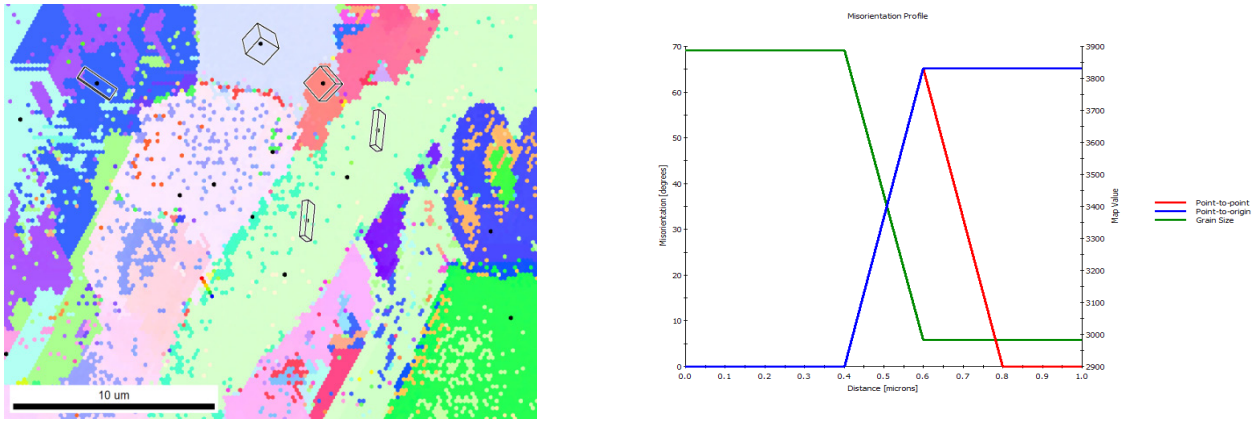

a) b)

Fig. 6. Specimen 1: a) map of relative orientation between individual crystals, at selected points showing local orientation of the elementary cell, b) misorientation of the crystal lattice between individual crystals along the line marked in Fig. 6a, between the grains of the α_c-AlFeMnSi phase and the grain of the β_H-AlFeMnSi phase

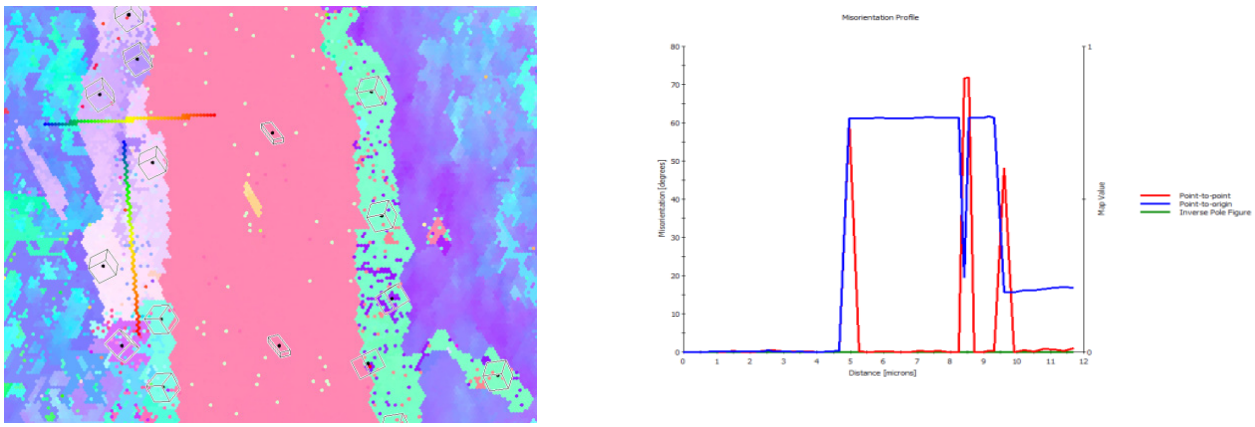

a) b)

Fig. 7. Specimen 2: a) map of relative orientation between individual crystals, at selected points showing local orientation of the elementary cell, b) misorientation of the crystal lattice between individual crystals along the line marked in Fig. 7a, between the α-Al solid solution, grains of the α_c-AlFeMnSi phase and the grain of the Al_3Fe phase

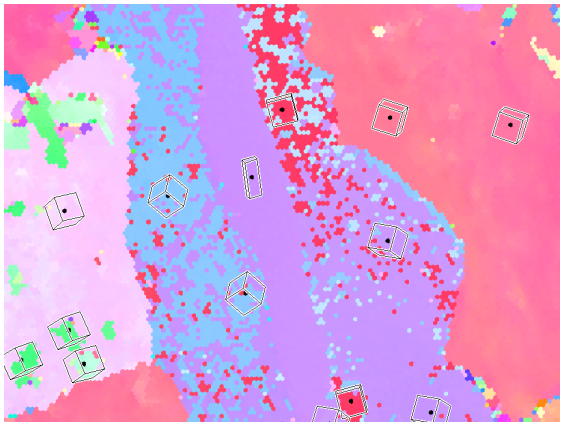

a)

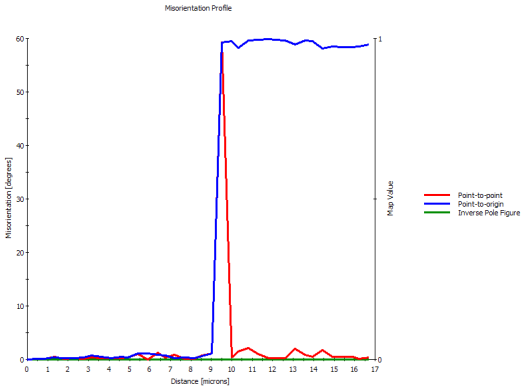

b)

Fig. 8. Specimen 3: a) map of relative orientation between individual crystals, at selected points showing local orientation of the elementary cell, b) misorientation of the crystal lattice between individual crystals along the line marked in Fig. 8a, between the grain of the α_c-AlFeMnSi phase and the grain of the Al_3Fe phase

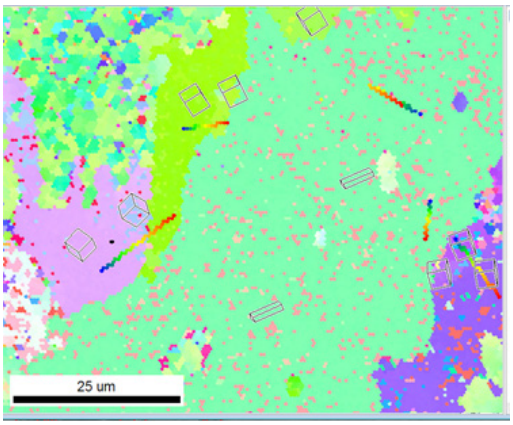

a)

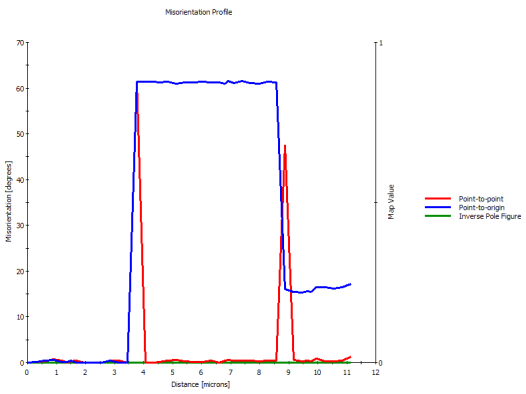

b)

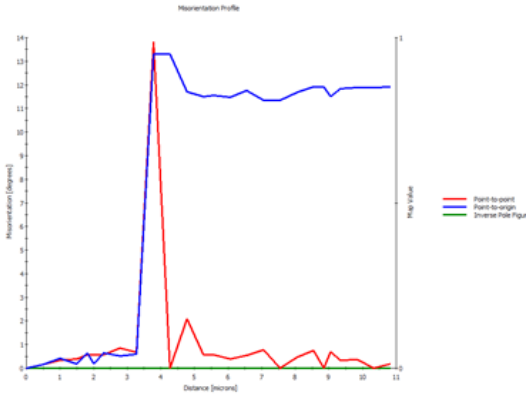

c)

Fig. 9. Specimen 4: a) map of relative orientation between individual crystals, at selected points showing local orientation of the elementary cell, b) misorientation of the crystal lattice between individual crystals along the line marked in Fig. 9a, between the α-Al solid solution, grains of the α_c-AlFeMnSi phase and grain of the Al_3Fe phase

The obtained results allowed the estimation of the misorientation angle between intermetallic phases crystals, depending on their crystal lattice and chemical composition (Table 4).

Table 4. Misorientation angle between selected phase crystals

No of specimen	Disorientation degree			
	Interface between phases, properitectic/ peritectic	Interface between properitectic/ α-Al solid solution	Sympathetic boundary	Grain boundary
1	30−70°	20−60°	15−30°	50−80°
2	70°	65°	20−30°	50−80°
3	50−70°	20−50°	10−30°	30−70°
4	30−80°	20−60°	15°	60−70°

The data in Table 4 were subsequently used in further considerations. Based on the estimated misorientation range between particular kinds of crystals, at interfaces α_c-AlFeMnSi/Al_3Fe, α_c-AlFeMnSi/Al, the procedure for indicating both phase and grain boundaries was tested and optimized. The procedure was based on the selection of the range of misorientation for a given interface, step by step, until obtaining its optimized value (Fig. 10). The criteria adopted for the initial analysis of the collected data in the orientation maps followed by their selection allowed the obtaining of results that represented the misorientation range of the crystal lattice for each interface.

5. Summary and conclusions

Procedures based on the application of commercial TEAM and OIM systems for collecting EBS diffraction patterns were applied to identify intermetallic phases in the microstructure of multicomponent, polyphase aluminum alloys.

Data collection parameters using SEM SCIOS, an EDAX X-ray microanalyzer and a Hikari camera, along with the acceptable range of their modification, were tested to determine the optimal analytical procedure.

The analysis focused on the data contained in phase and orientation maps as the source of information on the alloy microstructure, especially in two-phase microregions of peritectic crystallization involving the intermetallic phase, α_c-AlFeMnSi.

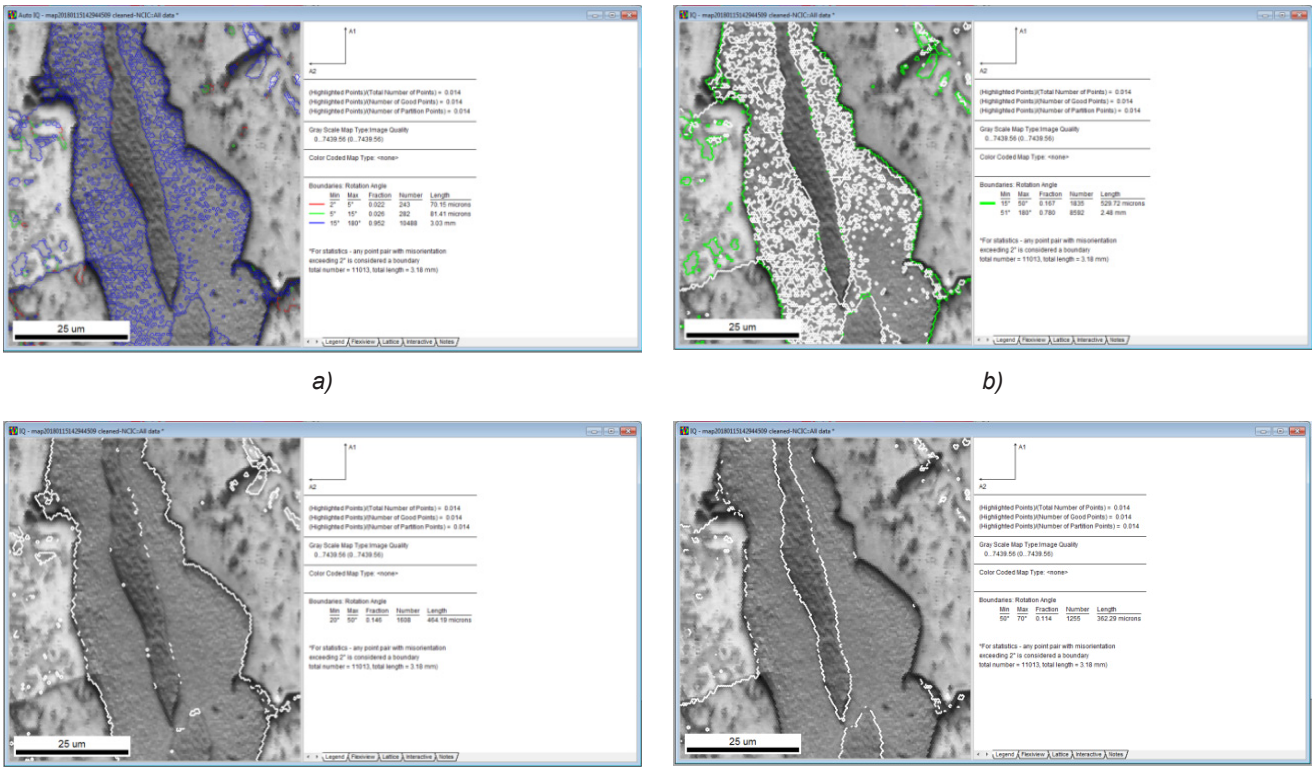

a) *b)*

c) *d)*

Fig. 10. Specimen 3. Estimation of the relative misorientation of the crystal lattice between crystalline phase grains in the selected microregion: a) initial result obtained using functions of the TEAM system, b−d) sequence of subsequent matches of misorientation degree at selected grain boundaries (b) and at interfaces α_c-AlFeMnSi/Al (c) and α_c-AlFeMnSi/Al_3Fe (d)

Although the data recorded for the particular specimen were rather dispersed, several kinds of typical interfaces could be identified (Table 4):

– Interface between intermetallic phases: properitectic/peritectic α_c-AlFeMnSi;

– Interface between matrix and intermetallic phase: α-Al solid solution / peritectic α_c-AlFeMnSi;

– Internal interface inside peritectic phase: 1) between layer of peritectic reaction product and semicongruent crystals of the α_c-AlFeMnSi phase, and 2) grain boundary between semicongruent crystals of the peritectic α_c-AlFeMnSi phase.

The range of the misorientation degree estimated for grain boundaries between different phases showed that they were rather high-angle boundaries. This is a result typical for phase constituents when an alloy macrostructure forms during endogenic solidification.

However, the misorientation ranges on the interfaces between intermetallic phases in two-phase microregions seem to indicate a possible effect of the degree of matching of the crystal structure and the local chemical composition (Fe/Mn ratio) of neighboring microregions on its value.

Assuming that the first crystals of the α_c-AlFeMnSi phase are formed as a result of heterogeneous nucleation on the surface of the peritectic phase crystals, the influence of the mutual matching of the crystal lattice of both phases (Eq. 1) can have a direct effect on the critical radius of nuclei r [8,9]:

$$r^3 = f\{d^{hkl}_{s/n} = \Sigma[([d_{uvw/s} \cos \upsilon - d_{uvw/n}])/d_{uvw/n}]/^3 \quad (1)$$

Thus, the low misorientation angle observed between the layer of the α_c-AlFeMnSi peritectic phase formed as a result of the peritectic reaction and the semi-congruent crystals of α_c-AlFeMnSi (Table 4) may confirm the assumption of their sympathetic nucleation at this stage of the peritectic process [2]. Based on the obtained results the geometrical relationships between peritectic cubic phase, α_c-AlFeMnSi, and properitectic crystals of both phases, β_H-AlFeMnSi (hexagonal) and Al_3Fe (tetragonal), could not be recognized. However, the data shown in Table 4 seem to indicate that, with an increase in the value of the Fe/Mn ratio, the tendency to reduce the range of misorientation at interface becomes apparent.

Thus, taking into account the results obtained from the examinations, the following conclusions can be formulated:

1. The EBSD analysis data in the form of point diffraction patterns and in the form of phase and orientation maps is a useful tool for the identification of processes on the alloy solidification path, especially in the initial stage of solid phase nucleation.

2. At this stage of the examinations the data concerning the identified range of crystal lattice misorientation at the interfaces and at grain boundaries in the aluminum alloy with the transition metals Fe and Mn, are rather qualitative. The quantitative description of the recognized relationships requires further research and should be confirmed based on a statistically significant dataset.

Acknowledgments

This work was realized with a financial support of the Polish Ministry of Industry and Development under FRI project No. 8003/00/2018.

References

1. Fraś E. 1992. *Krystalizacja metali i stopów (Crystallization of metals and alloys).* Warszawa: PWN.

2. Warmuzek M. 2014. *Krystalizacja perytektyczna w stopach AlFeMnSi.* Oficyna Wydawnicza Politechniki Rzeszowskiej.

3. Dubois J.-M. *Complex, metallic, and so different, properties and applications of complex intermetallics.* World Scientific Publishing Co. Pte. Ltd., http://www.worldscibooks.com/materialsci/7228.html.

4. StJohn D.H. 1990. „The peritectic reaction". *Acta Metallurgica et Materialia* 38 (4) : 631−636.

5. Shibata H., Y. Arai, M. Suzuki, T. Emi. 2000. „Kinetics of peritectic reaction and transformation in Fe-C alloys". *Metallurgical and Materials Transactions B* 31 (5) : 981−991.

6. Phelan D., M. Reid, R. Dippenaar. 2008. „Kinetics of the peritectic reaction in Fe-C alloy". *Materials Science and Engineering: A* 477 (1−2) : 226−232.

7. Warmuzek M., J. Sieniawski, K. Rabczak. 2005. „The course of the peritectic transformation in the Al-rich Al-Fe-Mn-Si alloys". *Journal of Materials Processing Technology* 162−163 (15 May 2005) : 422−428.

8. Trivedi R. 2005. „The role of heterogeneous nucleation on microstructure evolution in peritectic system". *Scripta Materialia* 53 (1) : 47−52.

9. Kundin J., H.-L. Chen, R. Siquieri, H. Emmerich, R. Schmid-Fetzer. 2011. „Investigation of the heterogeneous nucleation in a peritectic AlNi alloy". *The European Physical Journal Plus* 126 (96) : 1−18.

10. Orozco-González P., M. Castro-Román, S. Maldonado-Ruíz, S. Haro-Rodríguez, F. Equihua-Guillén, R. Muñiz-Valdez, S. Luna-Álvarez, M. Montoya-Dávila, A. Hernández-Rodríguez. 2015. „Nucleation of Fe-rich intermetallic phases on α-Al_2O_3 oxide films in Al-Si alloys". *Journal of Minerals and Materials Characterization and Engineering* 3 (1) : 15−25, http://dx.doi.org/10.4236/jmmce.2015.31003.

11. Warmuzek M., W. Ratuszek, G. Sęk-Sas. 2004. „Chemical inhomogeneity of intermetallic phases precipitates formed during solidification of the Al-Si alloys". *Materials Characterization* 54 (1) : 31−40.

12. Orozco-González P., M. Castro-Román, J. López-Cuevas, A. Hernández-Rodríguez, R. Muñiz-Valdez, S. Luna-Álvarez, C. Ortiz-Cuellar. 2011. „Effect of iron addition on the crystal structure of the a-AlFeMnSi phase formed in the quaternary Al-Fe-Mn-Si system". *Revista de Metalurgia* 47 (6) : 453−461, doi: 10.3989/revmetalm.1068.

13. Ferraro S., G. Timelli. 2015. „Influence of sludge particles on the tensile properties of die-cast secondary aluminum alloys". *Metallurgical and Materials Transactions B* 46 (2) : 1022−1034, DOI: 10.1007/s11663-014-0260-3.

14. *SEM-SCIOS FEI User Operation Manual*. 2016.

15. *EDAX TEAM User manual, Version 4.4*. 2016.

16. Raghavan V. 2007. „Al-Fe-Mn-Si (Aluminium-Iron-Manganese-Silicon)". *Journal of Phase Equilibria and Diffusion* 28 (2) : 215−217.

17. Raghavan V. 2007. „Al-Mn-Si (Aluminium-Manganese-Silicon)". *Journal of Phase Equilibria and Diffusion* 28 (2) : 192−196.

18. Orozco-González P., M. Castro-Román, A.I. Martínez, M. Herrera-Trejo, A.A. López, J. Quispe-Marcatoma. 2010. „Precipitation of Fe-rich intermetallic phases in liquid Al-13.58Si-11.59Fe-1.19Mn alloy". *Intermetallics* 18 (8) : 1617−1622.

19. Flores-Valdes A., J.A. Toscano, S. Rodríguez, A. Salinas, E. Nava-Vázquez. 2009. „Microstructure formation of Al-Fe-Mn-Si aluminides by pressure assisted reactive sintering of elemental powder mixtures". *Advanced of Materials Research* 68 : 21−33.